An In Vitro Analysis of the Influence of the Arterial Stiffness on the Aortic Flow Using Three-Dimensional Particle Tracking Velocimetry

U. Gülan[1], B. Lüthi[1], M. Holzner[1], A. Liberzon[2], A. Tsinober[2], and W. Kinzelbach[1]

[1] Institute of Environmental Engineering, ETH Zurich, Zurich, Switzerland
[2] School of Mechanical Engineering, Tel Aviv University, Tel Aviv, Israel

Abstract— **A three-dimensional pulsatile aortic flow in a human ascending aorta is investigated in-vitro in this paper. A non-intrusive measurement technique, 3D Particle Tracking Velocimetry (3D-PTV), has been applied to the anatomically accurate silicon replicas. A compliant and a stiff aortic model were analyzed to better understand the influence of the arterial stiffness. The realistic models are transparent which allows optical access to the investigation domain. Our results showed that increasing the arterial stiffness considerably increases the systolic velocity and hence mean kinetic energy. Quite strikingly, the turbulent kinetic energy is about one order of magnitude higher in the stiffer model during the deceleration phase which manifests that a blood element is exposed to higher shear stresses in the stiffer model. Moreover, we found that the compliant model introduces pressure oscillations during the diastolic phase which are associated with the Windkessel effect.**

Keywords— **3D-PTV, ascending aorta, image processing, arterial stiffness, Lagrangian flow field.**

I. Introduction

The aorta, which is the largest artery in the cardiovascular system, is the origin of the systemic circulation. It is a flexible artery with a high distensibility. The elastic walls allow the aorta to respond to the flow and pressure variations. During the systolic phase, the aorta stores almost half of the stroke volume ejected by the left ventricle by distending the walls. The stored blood is forwarded to the peripherial circulation contracting the arterial walls during the diastolic phase which is linked to the so-called "Windkessel effect" [1].

Stiffness is defined as the resistance to deformation [2]. Calcification and reduction in elastic fibers cause an increase in stiffness of the artery. Compliance is the inverse of stiffness and refers to the ratio of the change in volume to the pressure difference during the systolic and diastolic phases [1]. The compliance is a function of the wall properties, i.e. thickness, diameter and elastic modulus of the artery. Compliance of the aortic wall is thus believed to eminently influence the temporal and spatial evolution of the flow. Ageing and hypertension are claimed as the primary factors responsible for the increase in arterial stiffness [3]. From clinical point of view, measuring stiffness is a crucial marker as a predictor of cardiovascular morbidity [2]. Aortic stiffness may provoke abnormalities in blood flow in the cardiovascular system. It is found that aortic stiffness and atherosclerosis are highly correlated [4]. Accordingly, further analysis on the influence of the aortic stiffness on the aortic flow and the evolution of turbulent kinetic energy is needed to provide an informative and complimentary data for clinical purposes.

Phase Contrast Magnetic Resonance Imaging (PC-MRI) has been applied in-vivo and in-vitro to assess the flow field and turbulent velocity fluctuations. However, long scan times, low temporal resolution and low signal-to-noise ratio limits the capability of PC-MRI. Recently, 3D Particle Tracking Velocimetry (3D-PTV), an image based measurement technique, has been applied to extract the Eulerian and Lagrangian flow fields in an ascending aorta [5]. With the ability of 3D-PTV assessing flow velocities, velocity derivatives and Lagrangian trajectories simultaneously, it has become one of the standards for validation of in-vitro measurements [6].

The aim of this study is to shed a light on the influence of the aortic stiffness on the flow and fluctuating fields which can be translated into clinical application. For this purpose, 3D-PTV measurements were performed in anatomically realistic, rigid and compliant aortic replicas mimicking realistic flow conditions.

II. Method

3D-PTV is a non-intrusive measurement technique based on imaging of flow tracers. The experimental setup is explained in detail in the study of Gülan et al. [5]. Concisely, the experimental setup comprises an aortic replica, a Ventricular Assist Device (VAD, MEDOS, Germany) to mimic the function of the heart, a pneumatical pump system to drive the VAD and the optical part comprising a high speed camera (Photron SA5, Japan), an image splitter, mirrors and an Ar-Ion laser as light source as shown in Figure 1. The geometries of rigid and compliant aortic phantoms were obtained from high-resolution MRI scan of a healthy patient. The replicas were manufactured by Elastrat (Geneva, Switzerland). The high-speed camera was synchronized with the pump system to trigger the recordings in the beginning of every pulse. A novel dynamic calibration tool for image-based measurement

L.M. Roa Romero (ed.), *XIII Mediterranean Conference on Medical and Biological Engineering and Computing 2013,*
IFMBE Proceedings 41,
DOI: 10.1007/978-3-319-00846-2_5,

techniques, the so-called ”dumbbell calibration” was applied to calibrate the camera positions [5].

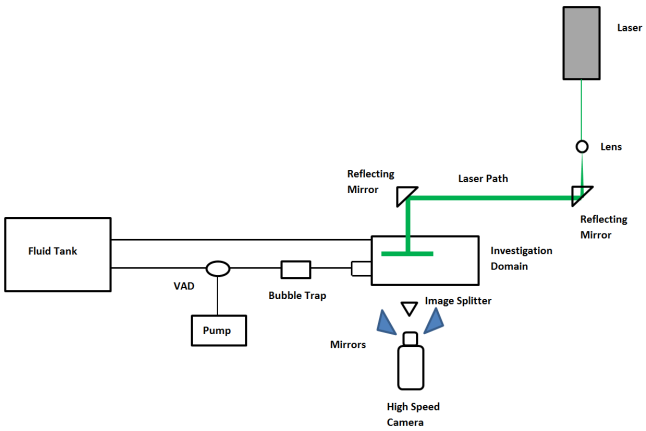

Fig. 1 Schematic view of the experiment setup [5]

3D-PTV allows to track particles in mediums with different refractive indexes. A mixture of glycerin, water and NaCl was used as working fluid to minimize the optical distortions by matching the refractive index of silicon. The parameters used in the measurements are presented in Table 1. In total, 35 heartbeats were recorded where a single heartbeat corresponds to a pulse length of 1.15s and data was phase averaged and mapped onto an Eulerian grid [5].

Table 1 Working fluid properties and flow parameters

Parameter	Unit	Rigid Model	Compliant Model
Stroke volume	ml	54	54
Density	g/cm^3	1.2	1.2
Viscosity	cm^2/s	4.85×10^{-6}	4.85×10^{-6}
Peak Reynolds number		3584	2323

III. Results

Aortic flow is a three-dimensional, complex and transitional flow. Generally, we found that pulsatility, the curved geometry of the aorta and its non-stationary boundaries induced a 3D flow with the presence of strong secondary flows. Figure 2 qualitatively describes the influence of arterial stiffness on the flow field. The comparison of Lagrangian trajectories along the compliant (left) and rigid (right) ascending aortas for a time interval of 0.1s during the deceleration phase is shown in Figure 2. As it is seen from the figure, the particle trajectories are mainly oriented along the axial direction and pronounced helical flow features are present at the inner wall in the compliant model. On the other hand, flow is more disorganized and coherent helical pattern vanishes in the rigid model which manifests that stiffness has considerable influence on the flow field.

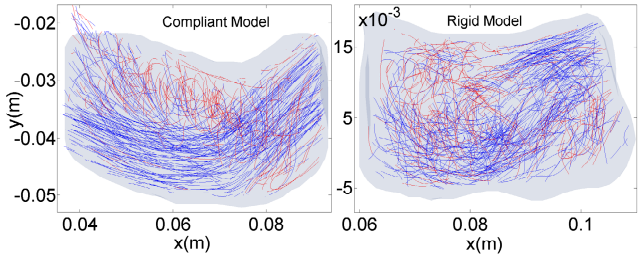

Fig. 2 Lagrangian trajectories along the compliant model (left) and rigid model (right) during the deceleration phase (Blue-coded trajectories refer to antegrade flow and the red-coded trajectories refer to retrograde flow)

Figure 3 shows the temporal behavior of the volumetric flux for the rigid and the compliant model. Both curves show a steep increase, peak and steep decrease during systole, where the peak value is higher for the rigid model. During diastole, there is a qualitative difference where the compliant model shows oscillations. These oscillations are due to the compliance of the walls, i.e. the aorta contracts and ejects fluid. This is analyzed in more detail in the following.

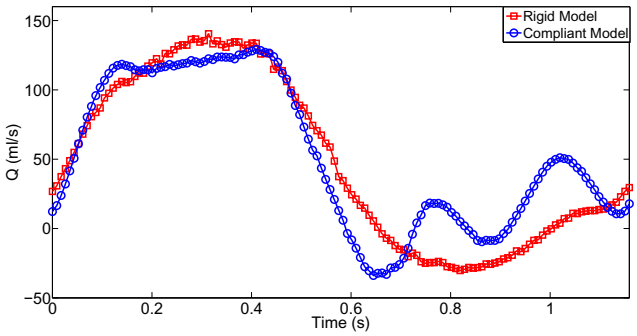

Fig. 3 Temporal evolution of phase averaged volumetric flux for both rigid and compliant models

To better understand the factors responsible for the flux oscillations, it is interesting to decompose the budget of the change of the volumetric flux. The variation of volumetric flux over time can be written as;

$$\underbrace{\frac{\partial Q}{\partial t}}_{\text{volumetric flux change}} = \frac{\partial AU}{\partial t} = U \underbrace{\frac{\partial A}{\partial t}}_{\text{areal change}} + A \underbrace{\frac{\partial U}{\partial t}}_{\text{local acceleration}} \quad (1)$$

where Q(x) is the volumetric flux, U(x,t) is the streamwise velocity averaged over the cross section, A(x,t) is the cross sectional area. The temporal change of cross sectional area is zero for the rigid model and hence the volumetric flux change is directly proportional to the local acceleration. As shown in Figure 4, the local acceleration is mainly responsible for the change in volumetric flux for the compliant model and the influence of the cross sectional change is negligible.

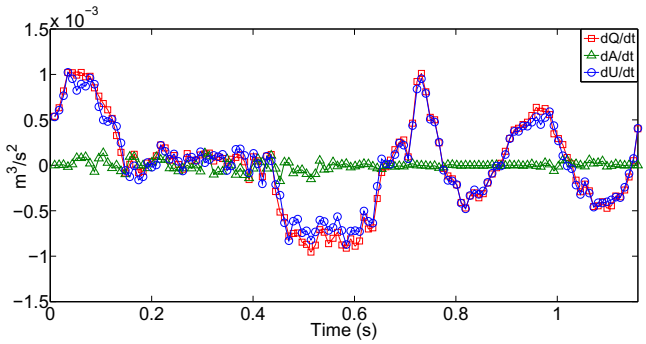

Fig. 4 Rate of the change of volumetric flux and its decomposition at the mid cross section of the compliant model

As we observed that local acceleration has dominant influence on the volumetric flux, it is logical to investigate the budget of local acceleration to highlight the factors responsible for the variation of the local acceleration. Accordingly, we analyze the phase averaged one dimensional Navier-Stokes equation averaged over the cross section.

$$\underbrace{\frac{\partial \tilde{U}}{\partial t}}_{\text{local acceleration}} = \underbrace{-\alpha\tilde{U}\frac{\partial \tilde{U}}{\partial x}}_{\text{convective term}} - \underbrace{\frac{1}{\rho}\frac{\partial \tilde{P}}{\partial x}}_{\text{pressure gradient}} - \underbrace{\tilde{\tau}_0/R_h\rho}_{\text{wall friction}} + \underbrace{gsin\theta}_{\text{gravitational acceleration}} \underbrace{-\frac{1}{A}\int \langle(\tilde{u}\cdot\nabla)\tilde{u}\rangle_\phi dA}_{\text{Reynolds stresses}} \quad (2)$$

where $\tilde{U}$ is the streamwise velocity component averaged over the cross section, $\tilde{P}$ is the pressure averaged over the cross section, g is the gravitational acceleration, $\tilde{\tau}_0$ is the wall shear stress, R_h is the hydrodynamic radius, $\tilde{u}$ is the turbulent fluctuating velocity, α is convective coefficient and the angle brackets denote the average over different pulses. We found that convective acceleration and pressure gradient terms have the strongest influence on the local acceleration. In Figure 5, we present the temporal evolution of local acceleration and convective acceleration for both rigid and compliant models.

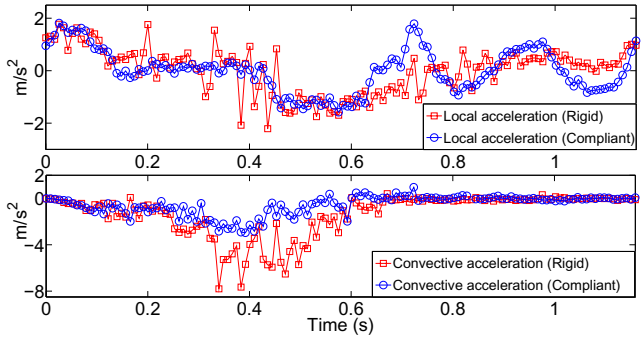

Fig. 5 Comparison of local and convective acceleration for the rigid and compliant models

As it is seen from the figure, local acceleration becomes negative during the deceleration phase by means of the existence of the retrograde flow for both models. During the diastole, the change in local acceleration is small in the rigid model which is consistent with Figure 3. Furthermore, we found that convective acceleration is higher during the systolic phase in the rigid model which is associated with the high mean velocity for the rigid model.

To provide a complimentary result to Figure 5, we exhibit the temporal evolution of pressure gradient for both models in Figure 6.

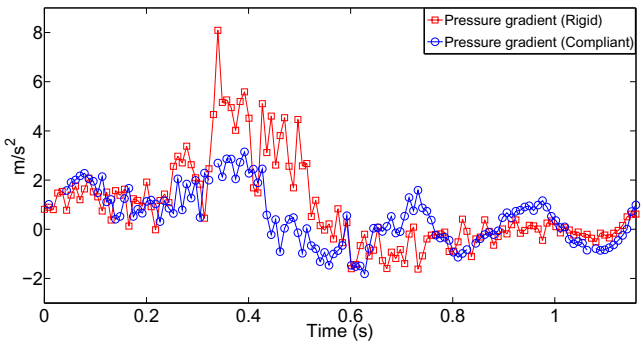

Fig. 6 Temporal evolution of pressure gradient for both models

Since there is no considerable change in convective acceleration during the diastolic phase (Figure 5, bottom), pressure gradient is responsible for the oscillations during the

diastole in the compliant model which is linked to the Windkessel effect. Moreover, rigid model shows higher pressure gradient during the systolic phase.

Cardiovascular flow is typically laminar. However, blood flow becomes turbulent in larger arteries such as aorta [5]. As turbulent flow induces higher shear stress on a blood element compared to the laminar flow, it is important to investigate the evolution of turbulent kinetic energy to estimate the transport inefficiency. We exhibit the temporal evolution of mean kinetic energy (MKE) and turbulent kinetic energy (TKE) averaged over the entire ascending aorta in Figure 7. It is seen that MKE in the rigid model is higher than that in the compliant model during peak systole which points that stiffness increases systolic velocity. Furthermore, TKE of the rigid model is about one order of magnitude higher than that of the compliant model during the deceleration phase when TKE reaches a maximum. It manifests that stiffer aorta provokes pronounced production of TKE.

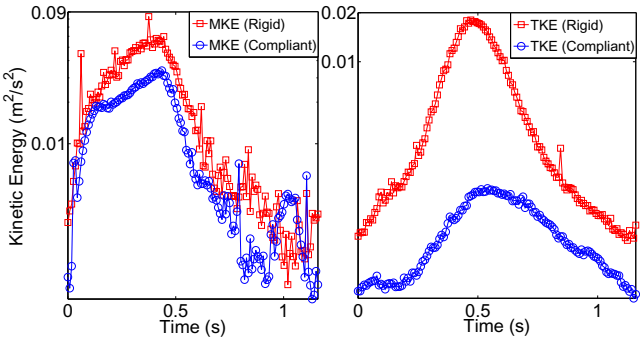

Fig. 7 Time evolution of mean turbulent kinetic energy (MKE) (left) and turbulent kinetic energy (TKE) (right) for both rigid and compliant models

IV. Conclusion

We presented an in-vitro investigation of the pulsatile aortic blood flow in an ascending aorta to highlight the influence of the arterial stiffness on the phase averaged and fluctuating velocity fields. An image-based measurement technique, 3D-PTV, has been applied to the anatomically realistic aortic replicas with matching index of refraction to avoid the optical distortions. Clinically realistic flow conditions have been mimicked. It is concluded that aortic distensibility plays a crucial role on the flow pattern. We found that increasing arterial stiffness decreases the influence of the Windkessel effect which is associated with the capability of blood storage of the peripheral flow during the systolic phase. We also observed that stiffer aorta leads to an increase in systolic velocity and hence an increase in convective acceleration and mean kinetic energy, a decrease in diastolic pressure gradient, an increase in systolic pressure gradient and less pressure oscillations during the diastolic phase. Analyzing the temporal evolution of the turbulent kinetic energy for two different models showed that the arterial stiffness noticeably increases turbulent kinetic energy during the entire heartbeat. The maximum turbulent kinetic energy level is reached during the deceleration phase for both models. A clear distinction between the rigid and the compliant models arises during the deceleration phase in terms of fluctuating velocities. The stiffer aorta introduces high fluctuating velocity and hence high production of turbulent kinetic energy. It is known that arterial stiffness is related to the atherosclerosis [2, 3, 4]. In the pathological flow conditions, red blood cells and platelets become more vulnerable as a result of high shear stress acting on a blood element. In future, this work will be extended towards the analysis of small scale stress analysis on a blood element to better understand the response of the cardiovascular system to the arterial stiffness.

Acknowledgements

This work was supported by ETH Research Grant ETH-24 08-2. Support from COST Action MP0806 is kindly acknowledged.

References

1. Belz G G. Elastic properties andWindkessel function of the human aorta Cardiovascular Drugs and Therapy. 1995;9:73-83.
2. Cavalcante J L, Lima J A C, Redheuil A, Al-Mallah M H. Aortic stiffness: current understanding and future directions Journal of the American College of Cardiology. 2011;57:1511-1522.
3. London G M, Guerin A P. Influence of arterial pulse and reflected waves on blood pressure and cardiac function Am Heart J. 1999;138:220-224.
4. Popele N M Van, Mattace-Raso F U, Vliegenthart R, et al. Aortic stiffness is associated with atherosclerosis of the coronary arteries in older adults: the Rotterdam Study Journal of Hypertension. 2006;24:2371-2376.
5. Gülan U, Lüthi B, Holzner M, Liberzon A, Tsinober A, Kinzelbach W. Experimental study of aortic flow in the ascending aorta via Particle Tracking Velocimetry Experiments in Fluids. 2012;53:1469-1485.
6. Knobloch V, Binter C, Gulan U, Boesiger P, Kozerke S. Assessment of 3D velocity vector fields and turbulent kinetic energy in a realistic aortic phantom using multi-point variable-density velocity encoding J Cardiovasc Magn Reson. 2012;14:W50.

Author: Utku Gülan
Institute: IfU, ETH Zurich
Street: Wolfgang Pauli Str-15, HIL G 34.2
City: Zurich
Country: Switzerland
Email: guelan@ifu.baug.ethz.ch